POLJOPRIVREDNA TEHNIKA
✧
Godina XXXVII
Broj 1, jul 2012.
Strane: 21 - 34

Poljoprivredni
fakultet
Institut za
poljoprivrednu
tehniku

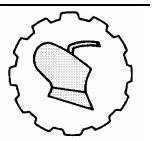

UDK: 631.372:669-8

Originalni naučni rad
Original scientific paper

3D DISCRETE ELEMENT MODEL TO DESCRIBE THE DRAFT FORCE AND THE INFLUENCES OF THE TOOL GEOMETRY

Tamás Kornél*, István J. Jóri

Budapest University of Technology and Economics, Faculty of Mechanical Engineering, Department of Machine and Industrial Product Design, Hungary

Abstract: Virtual DEM models were developed in correspondence with the real tests. In this article we will introduce the methods of how DEM approach was used in developing a model for the prediction of draught force on cultivator sweeps. The micro structure of soil is very complex and the conventional approach to explore the mechanical behavior of soil mainly relies on experimental shearing tests under laboratory conditions. The implementation of DEM is carried out by a series of numerical triaxial tests on granular assemblies with varying confining pressures and bond conditions. The results demonstrate that the numerical simulations can produce correct responses of the soil behavior in general, including the critical state response, as compared to experimental observations using the Mohr circles. The influences of cultivator sweep geometry was researched by DEM in 3D and were correlated with the soil bin tests results.

Key words*: soil, cultivator, DEM, modeling, tillage, soil bin, forces, 3D*

INTRODUCTION

The main function of the field cultivator is to prepare a proper seedbed for the crop to be planted into, to bury crop residue in the soil, to control weeds, and to mix and incorporate the soil to ensure the growing crop has enough water and nutrients to grow well during the growing season. Well-known that, the most influencing for the energetic requirement is the tool rake angel (β) (Fig 1.) and the operational velocity.

* Corresponding author: Műegyetem rkp. 3., H-1111 Budapest, Hungary.
E-mail address: tamas.kornel@gt3.bme.hu Tel.: +36-1/463-3505
This work is connected to the scientific program of the " Development of quality-oriented and harmonized R+D+I strategy and functional model at BME" project. This project is supported by the New Hungary Development Plan (Project ID: TÁMOP-4.2.1/B-09/1/KMR-2010-0002 and the TÁMOP - 4.2.2.B-10/1--2010-0009.)

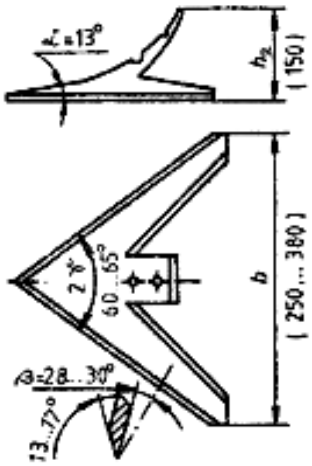

Figure 1. The Sweep-Tool geometry (2γ=63°, β=30°)

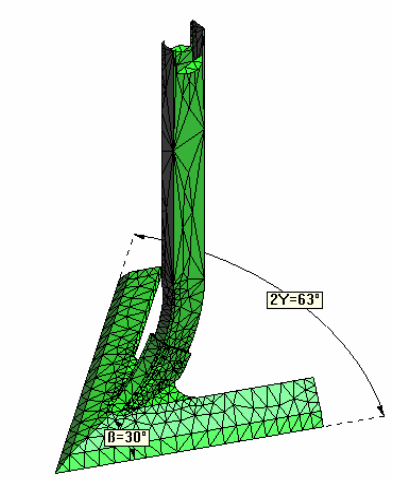

Figure 2. The mesh that define the sweep surface

MATERIAL AND METHODS

The study of soil-tool interaction is expensive and limited to certain cutting speeds [4]. As a result of the previous measurement in the soil bin study, some previous models were elaborated [5].

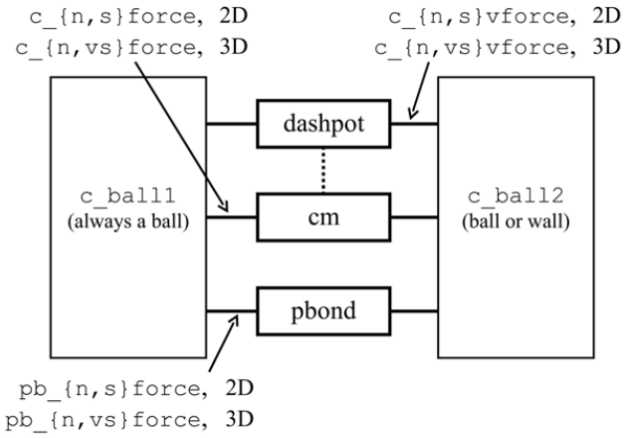

Figure 3. Components at a contact
(The cm and dashpot are always present.)
dashpot: global viscous damping
cm: contact model (linear, hertz…)
pbond: parallel bond

Description of the Parallel-Bond Model

The contact stiffnesses relate the contact forces and relative displacements in the normal and shear directions via and which are repeated here [1]. The normal stiffness is a secant stiffness:

$$F^n{}_i = K^n U^n ni \tag{1}$$

since it relates the total normal force to the total normal displacement. The shear stiffness is a tangent stiffness:

$$\Delta F^s{}_i = -k^s \Delta U^s{}_i \tag{2}$$

since it relates the increment of shear force to the increment of shear displacement.

PFC3D allows particles to be bonded together at contacts. The two standard bonding behaviors are embodied in contact bonds and parallel bonds. Both bonds can be envisioned as a kind of glue joining the two particles. The contact-bond glue is of a vanishingly small size that acts only at the contact point, while the parallel-bond glue is of a finite size that acts over either a circular or rectangular cross-section lying between the particles. The contact bond can transmit only a force, while the parallel bond [7] can transmit both a force and a moment:

$$\overline{F}_i = \overline{F}_i^n + \overline{F}_i^s \tag{3}$$

$$\overline{M}_i = \overline{M}_i^n + \overline{M}_i^s \tag{4}$$

where $\overline{F}_i^n$, $\overline{M}_i^n$ and $\overline{F}_i^s$, $\overline{M}_i^s$ denote the normal and shear component vectors, respectively. These vectors are shown in Fig. 4., where the parallel bond is depicted as a cylinder of elastic material.

Particles may be bonded only to one another; a particle may not be bonded to a wall. Both types of bonds are also created between all proximate particles within the given range, regardless of whether a normal force exists between them.

A parallel bond can be envisioned as a set of elastic springs with constant normal and shear stiffnesses, uniformly distributed over either a circular or rectangular cross section lying on the contact plane and centered at the contact point. These springs act in parallel with the point-contact springs that are used to model particle stiffness at a point, and whose constitutive behaviour. Relative motion at the contact (occurring after the parallel bond has been created) causes a force and a moment to develop within the bond material as a result of the parallel-bond stiffnesses. This force and moment act on the two bonded particles and can be related to maximum normal and shear stresses acting within the bond material at the bond periphery. If either of these maximum stresses exceeds its corresponding bond strength, the parallel bond breaks.

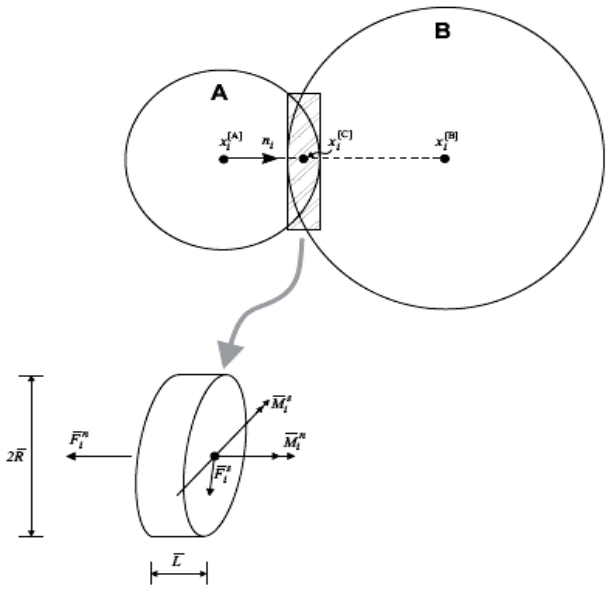

Figure 4. Parallel bond depicted as a cylinder of cementations material

A parallel bond is defined by the following five parameters: normal and shear stiffness k_n and k_s [stress/displacement]; normal and shear strength σ_c and τ_c[stress]; and bond radius R.

Mechanical Damping

Energy supplied to the particle system is dissipated through frictional sliding. However, frictional sliding may not be active in a given model or, even if active, may not be sufficient to arrive at a steady state solution in a reasonable number of cycles.

Local damping and viscous damping are available in PFC3D to dissipate kinetic energy. Local damping acts on each ball, while viscous damping acts at each contact. Local damping applies a damping force, with magnitude proportional to unbalanced force, to each ball. Viscous damping adds normal and shear dashpots at each contact [2]. These dashpots act in parallel with the existing contact model, and provide forces that are proportional to the relative velocity difference between the two contacting entities (ball-ball or ball-wall).

MATERIALS AND METHODS

The material properties and the iteration process in DEM

Using the results of the triaxial test (the peak strength and confining stress) we defined the Mohr's circles. Touching the circles we drew the Coulomb line. The angle of

the line and the x axis we defined the internal friction angle. The intersection of the Coulomb line and the y-axis we defined the cohesion.

Shear Box Test

At first we generated an aggregation, with that we had to evaluate and measure the effective bearing with the shear box test. In the test result we can define the aggregation properties as soil after the real soils mechanical parameters. It is a useful method for the comparison.

Table 1. The moisture content of the sample

The moisture content of the sand:			
Dry ing temperature: 105 ºC *Drying time: 2 hour*		$N = \frac{m_1 - m_2}{m_2} \cdot 100 \ [\%]$	
Sample	*Mass (before drying)*	*Mass (after drying)*	*Moisture content*
	m_1	m_2	N
	(g)	*(g)*	*(mass %)*
1	*149*	*139*	*7,19*
2	*152*	*143*	*6,29*
3	*128*	*121*	*5,79*
4	*148*	*139*	*6,47*
5	*128*	*121*	*5,79*
Average:	*141*	*132,6*	*6,33*

At first, we must determine the relevant behaviors of our intended physical material, and then choose the appropriate microproperties by means of a calibration process in which the responses of the synthetic material are compared directly with the relevant measured responses of the intended physical material.

A series of shear box tests were performed (Fig. 6.). The simulated mechanical behavior of granular materials is compared with those observed from the laboratory tests.

$$Tf = cA + N \tan \varphi \tag{5}$$

where:
A - the area of the sample,
c - the cohesion of the material,
φ - its friction angle.

This is called the Mohr-Coulomb failure criterion. If the stress circle is completely within the envelope no failure will occur, because on all planes the shear stress remains well below the critical value.

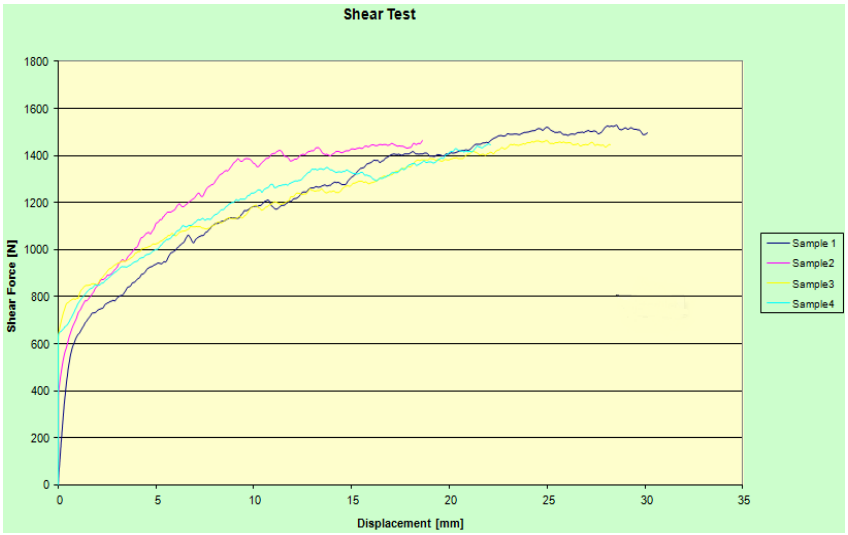

Figure 5. The Shear Box Test Results

The material properties and the iteration process in DEM

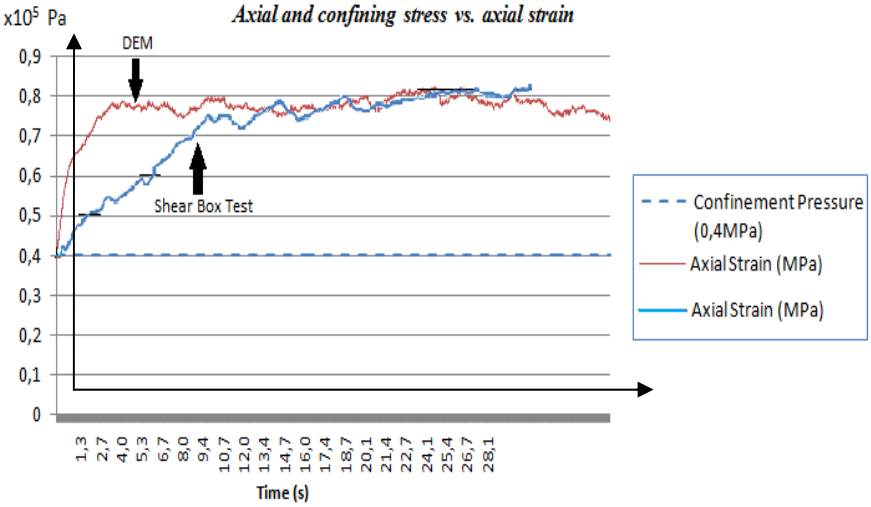

Figure 6. Axial and confining stress vs. axial strain (Triaxial Test and Shear Box Test Comparison) (CP=0,4MPa)

We can see on the Fig. 6. the resulted peak strength dependence of the confining pressure (P_c). For codes such as PFC that synthesize macro-scale material behavior from the interactions of microscale components, the input properties of the microscopic constituents are usually not known [3].

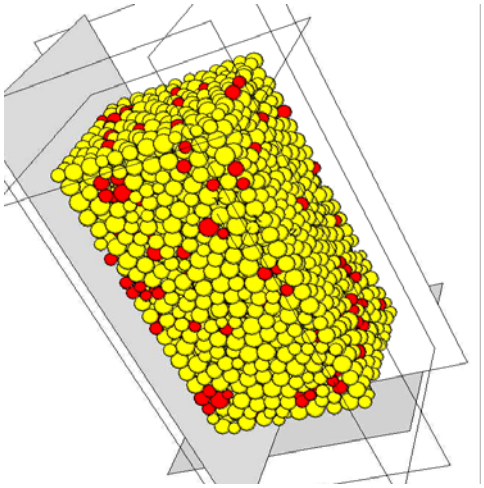

Figure 7. The TRIAXIAL TEST Process (PFC3D)

Although it is relatively easy to assign chosen properties to a PFC model, it is often difficult to choose such properties so that the behavior of the resulting synthetic material resembles that of an intended physical material.

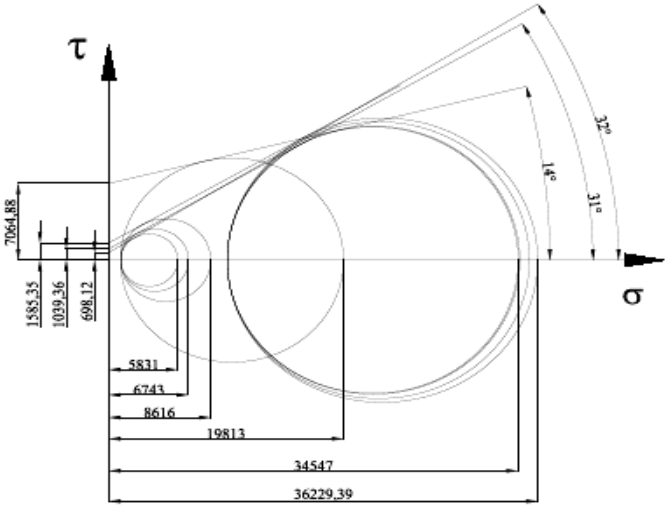

Figure 8. The Triaxial Test Result that define the soil mechanical parameters
(Φ = 32°, C = 7064,88 Pa)

For codes such as PFC that synthesize macro-scale material behavior from the interactions of microscale components, the input properties of the microscopic constituents are usually not known.

Table 2. The results of the triaxial tests

SPECIMEN (Iteration Process)		Triaxial Test Result 1.	Triaxial Test Result 2.	Triaxial Test Result 3.	Triaxial Test Result 4.
x: pack	y: Pc	sig_f	sig_f	sig_f	sig_f
	($x10^3$Pa)	($x10^4$Pa)	($x10^4$Pa)	($x10^4$Pa)	($x10^4$Pa)
1	1	0,6737	0,8616	0,5832	0,6317
1	10	3,6285	3,6201	3,5496	3,4945
	Cohesion (Pa)	698	1585	1039,36	7065
	Internal Friction Angle (Φ)	32°	31°	31°	14°
	Friction	0,3	0,5	0,5	0,5
	pb_rad	1	1	1	1
	pb_kn	1,5e2	1e4	1e4	0,3e6
	pb_ks	2,5e2	1e2	1e2	0,3e3
	pb_nstren	1e3	1e5	1e2	1e5
	pb_sstren	1e2	1e3	1e1	1e3

As we can see on the Figure 8. the cohesion is 7067,88 Pa and the internal friction angle is 32°. This soil mechanics property following the real triaxial tests is a kind of sand. With this process we can harmonize the real and the numerical methods.

Table 3. Model parameters

Parameter in DEM	Value
Bulk density (kg/m^3)	1850
Particle shape	Ball
Normal spring coefficient (K_n) [$N \cdot m^{-1}$]	1,00E+06
Tangential spring constant (K_s)[$N \cdot m^{-1}$]	1,00E+03
Coulomb damping (μ_g)	0,3
Friction coefficient between particles(μ)	0,3
damp viscous normal [$N_s \cdot m^{-1}$]	0,2
damp viscous shear [$N_s \cdot m^{-1}$]	0,2
Particle radius distribution [mm]	23,44-39,07
Friction coefficient between particle and the sweep tool	0,6
Void ratio	0,35
Parallel-Bond (heavy soil) (Result of the sinthezis)	
pb_rad	1
pb_kn ($Pa \cdot m^{-1}$)	0,30E+06
pb_ks ($Pa \cdot m^{-1}$)	0,30E+03
pb_nstren ($Pa \cdot m^{-1}$)	1,00E+05
pb_sstren ($Pa \cdot m^{-1}$)	1,00E+03
Time step of the calculation (Δt) (s)	4.0 × 10-5

The triaxial-test results presented in Tab. 2. The information was obtained from the functions as we can see on the Fig. 7. the axial and confining stress vs. axial strain. We can see the similarity of the Shear Box Test and the Triaxial Test Parameters and can use in our test these micro parameters (Fig. 6.). The soil samples were from the Soil Bin.

With these results we can draw the Mohr's circles, that's tangential line define the cohesion and the internal friction angle. In our research these two soil parameters are enough to define the material and we used these data in the iteration process (Fig. 8.).

Table 4. Key for the shear strength parameters

Soil type	*c (kN m^{-2})*	*φ (°)*	*tan φ*
sandy gravel	*0*	*31*	*0,601*
sand, slighty silty	*20*	*32*	*0,625*
silty sand	*30*	*29,5*	*0,566*
silty fine sand	*15*	*30*	*0,577*
sandy silt	*50*	*30*	*0,577*
clay, w=50%	*65*	*27*	*0,508*
moist clay	*80*	*22*	*0,404*
clay 50%<w<70%	*120*	*16*	*0,286*
clay w>70%	*170*	*20*	*0,364*

RESULTS AND DISCUSSION

The CAD support and the loosening process by DEM

To design and build the sweep tools we used the CAD support function. *PFC3D* is valued for its ability to model complex physics. While *PFC3D* offers many options for defining walls, creating complex walls with *PFC3D* may become tedious at times.

In *PFC3D*, the orientation of the walls determines the side the particles will interact with. The original normal vectors of each triangle in the model (each normal is represented at the center of gravity of each triangle).

The dynamic behavior of cohesive soils during the loosening process by a cultivator sweep was simulated by using the above established DEM mechanical model. The initialization of the interaction between the tool and cohesive soils is the complete model. The model is composed of discrete particles of different sizes. The parallel bonds produce cohesive forces between discrete particles, so parts of discrete particles are conglomerated and form particle aggregate clusters after the tillage process. The complete model is formed by bonding of elements in wide sizes. This structure of the model is similar to that of the actual cohesive soils.

We can see on the Fig. 10. the front of the sweep the parallel bond lines represent the compacted zone and the resulted forces between the particles [2].

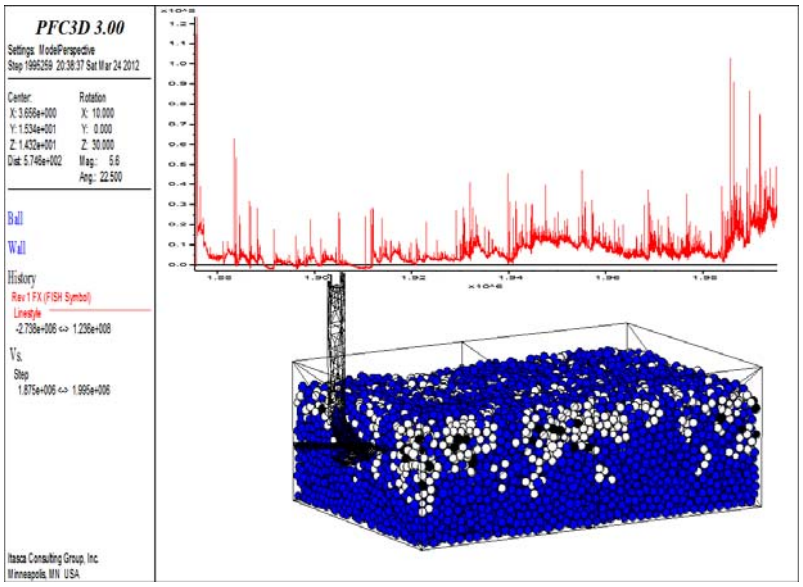

Figure 9. The soil (DEM) and the tool draft force under process
3D view of the TEST structure. Tool in 12 cm depth. (Soil Bin sizes: 2m x 1m x 0,8m)

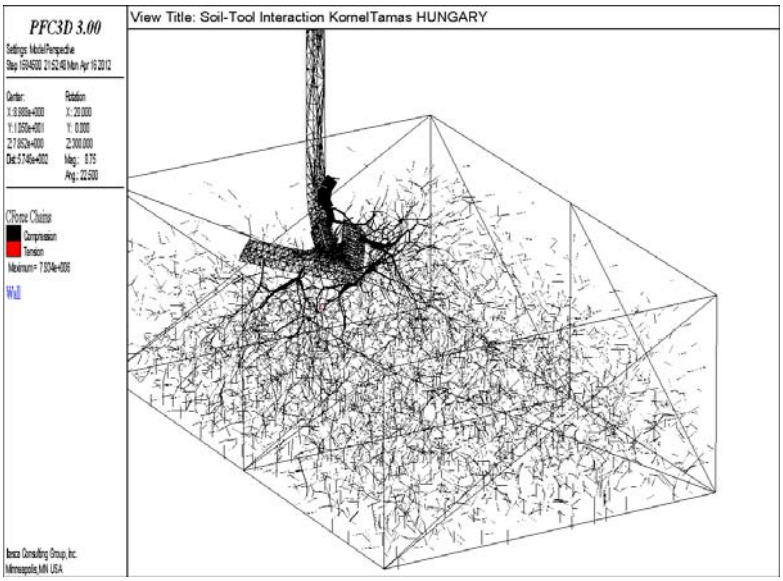

Figure 10. The force structure under the loosening process

As we can see on the Fig. 11. the DEM Draft Force is similar to the measured Soil Bin draft force. The difference could be the sampling accuracy and the noise of the soil bin cart.

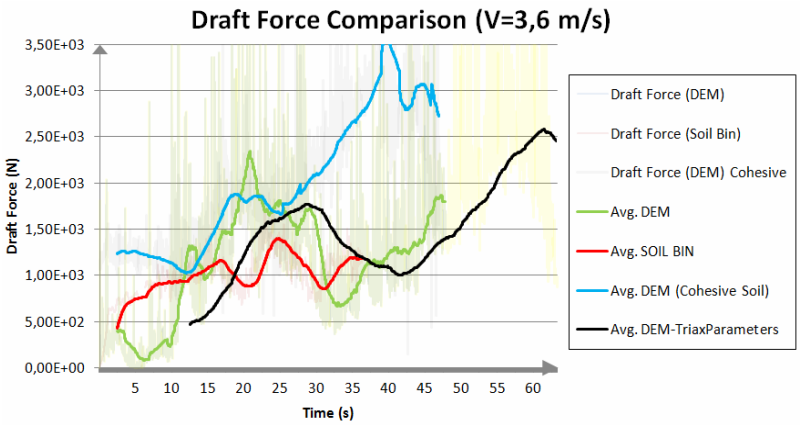

Figure 11. The Draft Force Comparison in 12cm depth and V=3,6m/s

With the CAD support function we imported the real accurate tool geometry. Under the measuring process a „routine" cumulating the draft force x components. With this routine we can measure other tillage tool draft forces.

The influence of the speed and the rake angle

The parallel-bond contact was used to describe the behavior of the cohesive soil (discontinuous) during soil-tool interface process.

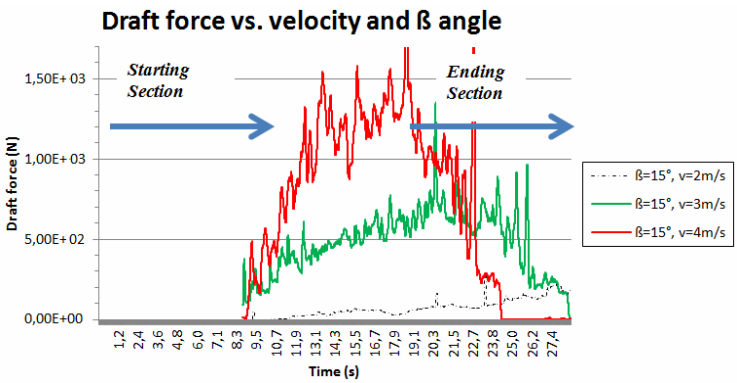

Figure 12. The influence of the speed (2,0-4,0 m/s) by DEM (ß=15°) in 20 cm depth

A series of models were analyzed with various soil properties, speed and rake angles using PFC3D Code (Fig. 12.). The results showed the significant effect of the tool rake angles and working speed on cutting forces in 20 cm depth (Figure 13.). In this research between the two extremities (2.0 - 4.0 m/s and, 5°-30°) the results are parabolic (Fig. 14.).

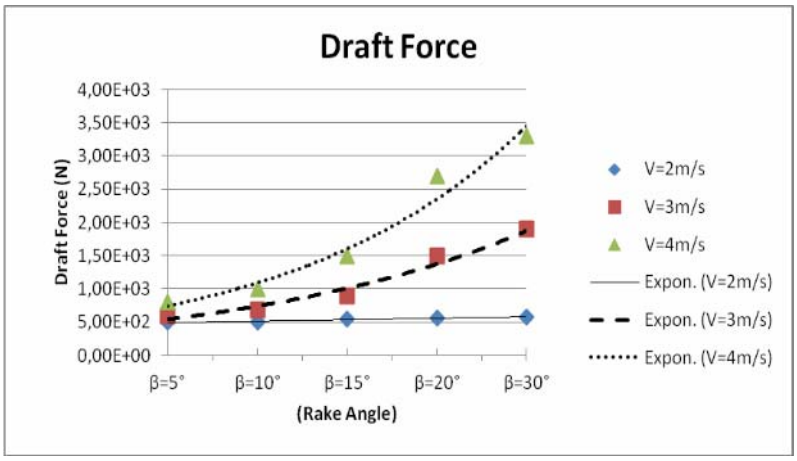

Figure 13. The Draft Forces rake angle (ß) and speed dependences in 20 cm depth

During the simulated tillage process by a cultivator sweep, soil evolves from the extrusion between soil clumps, the humping ahead of the tillage tool, and the climb along the surface of the sweep, to the rupture and separation of cohesive soil cluster

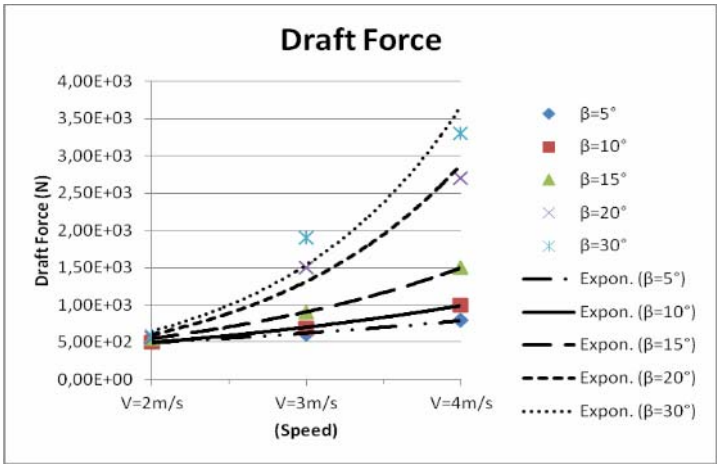

Figure 14. The Draft Forces speed and rake angle dependences in 20 cm depth

CONCLUSIONS

In this three dimensional discrete element analyses we carried out the simulation of the soil-tool interaction in agricultural soil and compared with a Soil Bin Test results. After the triaxial test method with which we validated the micro properties, a series of models were analyzed with various soil properties, speed and rake angles using in the three dimensional models. The results showed the significant effect of the tool working speed on cutting forces in 20 cm depth. In case the set of the appreciable parameters in

DEM synthetic material with parallel- bonds between the particles, we can synchronizing the virtual triaxial test (microproperties) and could be compared directly with the measured response of the physical material. The real soil macroproperties are the cohesion and the friction angle that we got from the science articles. With the parallel bonds we can model the cohesion. To use this method the Soil-Tool Interaction Model is well build to use other tool geometries.

The model can be used in development procedures of soil loosening tools for agricultural machines and technology, reducing the number of soil bin and field test.

BIBLIOGRAPHY

[1] Bojtár, I., Bagi, K. 1989. Analysis of the Satake- and Cundall-Parameters of Granular Material sin Non-Linear State-Changing Processes. In *Powders and Grains*, pp. 275-278. J. Biarez and R. Gourvés, Eds. Rotterdam: A. A. Balkema.

[2] Cundall, P. A. 1971. A Computer Model for Simulating Progressive Large Scale Movements in Blocky Rock Systems. In *Proceedings of the Symposium of the International Society of Rock Mechanics (Nancy, France, 1971)*, Vol. 1, Paper No. II-8.

[3] Mouazen, A.M., Neményi, M. 1996. Two-dimensional finite element analysis of soil cutting by medium subsoiler. *Hungarian Agric. Eng*. 9/96 32-36.

[4] Sitkei, Gy. 1967. A mezőgazdasági gépek talajmechanikai problémái. *Akadémiai Kiadó,* Budapest.

[5] Tamás, K., Jóri, J.I. 2008. Measuring Cart Development for Soil Bin Test. Soil Tillage – New Perspectives. *Book of Abstract, ISTRO, Branch.* Czech Republic, 5th International Conference, Brno pp. 41

[6] Tanner, D. 1960. Further Work on the Relationship between Rake Angle and the Performance of simple Cultivation Implements. *J. of Agr.Eng.Res*. 3.

[7] *PFC2D.* 2002. *Particle Flow Code in 3 Dimensions. Manual*, Version 3.0, Itasca Consulting Group, Inc., Minneapolis, 2002.

3D DISKRETNI MODEL VUČNE SILE I UTICAJA GEOMETRIJE RADNOG TELA

Tamás Kornél, István J. Jóri

Univerzitet za tehnologiju i ekonomiju Budimpešta, Mašinski fakultet,
Institut za mašine i industrijski dizajn, Budimpešta, Mađarska

Sažetak: Virtualni DEM modeli su bili razvijani uporedo sa realnim testiranjem. U ovom radu ćemo predstaviti metode pristupa DEM u razvoju modela za predviđanje vučne sile na krilima kultivatorske motičice. Mikro struktura zemljišta je veoma kompleksna, a konvencionalni pristup istraživanju mehaničkog ponašanja zemljišta većinom se oslanja na eksperimentalne testove u laboratorijskim uslovima. Primena

DEM je izvedena serijama numeričkih triaksialnih testova na granularnim podlogama sa različitim pritiscima i uslovima u bazenu. Rezultati pokazuju da numeričke simulacije generalno mogu korektno da predvide ponašanje zemljišta, uključujući reakciju na kritično stanje, u poređenju sa eksperimentalnim istraživanjima upotrebom Mohr krugova. Uticaji geometrija krila kultivatorske motičice su istraživani upotrebom DEM u 3D i poređeni sa rezultatima testova u zemljišnom bazenu.

***Ključne reči**: zemljište, kultivator, DEM, modeliranje, obrada, zemljišni bazen, sile, 3D*

Datum prijema rukopisa: *Paper submitted:*	04.05.2012.
Datum prijema rukopisa sa ispravkama: *Paper revised:*	
Datum prihvatanja rada: *Paper accepted:*	04.06.2012.